the balance between LXRα and FXR actions may lead to the diverse effects of dietary cholesterol on CYP7A1 expression between the species.

C57BL/6 mice have been identified as being susceptible to the development of atherosclerosis under a diet containing cholesterol, high fat, and cholic acid [12,13]. Without dietary cholic acid, however, the animals do not develop early atherosclerosis. Although atherosclerosis in the model has been widely studied, the effects of those dietary components on LXRα and FXR activation are not fully understood. To address this issue, we measured mRNA expression of LXRα and FXR target genes, including CYP7A1 gene, in the livers of C57BL/6 mice fed diets containing cholesterol, high fat, and/or cholic acid. Surprisingly, unlike the observations in rats [5,10,14], dietary cholesterol with or without high fat did not affect CYP7A1 mRNA level whereas cholic acid with or without cholesterol + high fat greatly reduced its transcript level. Our results suggest that FXR dominantly regulates CYP7A1 transcription in the atherogenic diet-fed mice.

2. Materials and methods

2.1. Animals and treatments

Male C57BL/6 mice were obtained from Japan SLC (Hamamatsu, Japan) at 7 weeks of age and maintained under a specific pathogen-free condition with controlled temperature and humidity and a 12-h light/12-h dark cycle. Mice were given a standard laboratory diet (CE-2; CLEA Japan, Tokyo, Japan) and water ad libitum. After a 7-day acclimation period, animals were divided into the following five groups: (a) controls fed CE-2 (control, $n=8$), (b) mice fed CE-2 supplemented with 0.5% sodium cholate (CA, $n=7$), (c) mice fed CE-2 supplemented with 2% cholesterol (Cholesterol, $n=8$), (d) mice fed an atherogenic diet containing 1.25% cholesterol, 7.5% cocoa butter, 7.5% casein, and 0.5% sodium cholate (AT, $n=5$) [15], and (e) mice fed the diet equivalent to AT with the omission of sodium cholate (AT − CA, $n=5$). The experimental diets were fed ad lib for 2 weeks and thereafter, blood and liver samples were obtained from the mice at 2 p.m. without artificial fast because it may affect mRNA expression of various genes [16]. All animal procedures were preformed in accordance with the Guideline for Animal Research at Jichi Medical School.

2.2. Lipid measurements

Enzymatic assays for total cholesterol, triglycerides, and total bile acids were performed using kits purchased from Wako Pure Chemical Industries (Osaka, Japan). HDL cholesterol was measured using the Choletest N HDL Kit (Daiichi Pure Chemicals, Tokyo, Japan). The intra- and inter-assay coefficients of variation were all <1% for total cholesterol and triglycerides, 4.8% and 10.8% for total bile acids, and 0.4% and 1.6% for HDL cholesterol, respectively. LDL + VLDL cholesterol concentrations were determined as the difference between total and HDL cholesterol concentrations. For hepatic cholesterol and triglyceride determinations, lipids were extracted using 100 mg of tissue as described [17].

2.3. RNA extraction and real-time quantitative PCR

The isolation of total RNA was achieved using the RNeasy Mini Kit according to the manufacturer's instructions (Qiagen, Valencia, CA). Reverse transcription was done by 1.2 μg of total RNA, random hexamer primer and RevertAid M-MuLV reverse transcriptase (Fermentas, Hanover, MD). The resulting cDNA equivalent to 60 ng of RNA was used for the real-time quantitative PCR, performed with the ABI Prism 7700 Sequence Detection System (Applied Biosystems, Foster City, CA), as previously described [18]. All of specific sets of primers and TaqMan probes in the present study were obtained from Applied Biosystems (Assays-on-Demand Gene Expression Products and TaqMan Rodent GAPDH Control Reagents).

All primer sets except that of TaqMan Rodent GAPDH Control Reagents were designed to be located in two exons to avoid the amplification of potentially contaminating genomic DNA. To control for the variation in the amount of DNA available for PCR in the different samples, gene expressions of the target sequence were normalized in relation to the expression of an endogenous control, glyceraldehyde-3-phosphate dehydrogenase (GAPDH). Because the efficiency of the target amplification was approximately equal to that of the GAPDH amplification, data were analyzed using comparative threshold cycle method [19]. The intra- and inter-assay coefficients of variation of the relative expression values were generally <20%, and we considered the mean relative values of less than 0.8 or more than 1.2 to be significant in this study.

2.4. Statistics

Data were analyzed using the Mann–Whitney U test or one-way analysis of variance with a post-test of Fisher's protected least significant differences. Values are presented as the mean ± S.E., and a P value of less than 0.05 was considered significant. All calculations were performed using the computer program StatView, version 5.0 (SAS Institute, Cary, NC).

3. Results

3.1. Effects of atherogenic diet components on serum lipid and bile acid, and hepatic lipid concentrations

To investigate the effects of atherogenic diet components on serum and hepatic lipid concentrations, C57BL/6 mice were fed diets containing cholesterol, high fat, and/or cholic acid for 2 weeks. As shown in Table 1, Cholesterol (cholesterol alone) diet did not affect serum cholesterol concentra-

Table 1
Effects of atherogenic diet components on serum lipid and bile acid, and hepatic lipid concentrations

	Control	CA	Cholesterol	AT – CA	AT
Serum lipids and bile acids					
n	8	7	8	5	5
Total cholesterol (mg/dl)	74 ± 2	110 ± 9†	82 ± 2	134 ± 6†	188 ± 10†
LDL + VLDL cholesterol (mg/dl)	14 ± 2	71 ± 5†	26 ± 3*	48 ± 2†	125 ± 8†
HDL cholesterol (mg/dl)	60 ± 1	39 ± 4†	56 ± 2	86 ± 5†	63 ± 3†
Triglyceride (mg/dl)	59 ± 4	19 ± 2†	39 ± 6**	61 ± 11	9 ± 1†
Total bile acids (μmol/l)	6	84 ± 17**	5	4	65 ± 17**
Hepatic lipids					
n	8	5	5	5	5
Hepatic cholesterol (mg/g tissue)	2.5 ± 0.1	4.5 ± 0.3**	5.3 ± 0.3†	5.9 ± 1.0†	10.6 ± 0.4†
Hepatic triglyceride (mg/g tissue)	7.7 ± 0.9	6.9 ± 0.4	16.0 ± 1.6†	15.9 ± 2.0†	8.9 ± 0.8

Male C57BL/6 mice were fed each diet for 2 weeks, after which serum lipid and bile acid, and hepatic lipid concentrations were measured. Data are mean ± S.E. or maximum values. Control, a regular diet; CA, 0.5% sodium cholate; Cholesterol, 2% cholesterol; AT, an atherogenic diet; AT – CA, the diet equivalent to AT with the omission of sodium cholate.

* $P<0.05$, ** $P<0.01$, † $P<0.001$ vs. control.

tion while AT – CA (cholesterol + high fat) diet significantly increased this variable. On the other hand, serum cholesterol concentration increased 1.5-fold on CA (cholic acid alone) diet, and adding cholic acid to AT – CA diet (i.e., AT diet) induced further increase. These changes were not caused by the changes of HDL cholesterol, but by the increases in LDL + VLDL cholesterol both on CA and on AT diet. On AT – CA diet, however, both LDL + VLDL and HDL cholesterol significantly increased. Interestingly, feeding cholic acid (i.e., CA or AT diet) greatly reduced serum triglyceride concentrations. Additionally, serum bile acid concentrations rose only in mice fed cholic acid. These results suggest that both dietary components of cholic acid and cholesterol + high fat are necessary for changing circulating lipid concentrations to a large extent in mice.

Consistent with serum concentrations, hepatic cholesterol concentrations were elevated about two-fold on CA, Cholesterol, and AT – CA diets, and further increased to 4.3-fold on AT diet. In regard to hepatic triglyceride, the concentrations increased 2.1-fold both on Cholesterol and on AT – CA diet while CA diet did not affect this variable. Addition of cholic acid to AT – CA diet (i.e., AT diet) completely blunted the increase of hepatic triglyceride by cholesterol and/or high fat.

3.2. Effects of atherogenic diet components on mRNA expression of the LXRα regulated target gene

We next measured hepatic mRNA expression levels of ATP-binding cassette transporter (ABC) A1 gene, one of LXRα target genes [1,18,20], to evaluate the activation state of LXRα. ABCA1 is thought to be involved in the reverse cholesterol transport pathway by transporting intracellular cholesterol and phospholipids to cell surface-bound apolipoproteins and forms nascent HDL [20]. In concordance with circulating and hepatic cholesterol concentrations, CA, AT – CA, and AT diets significantly increased the transcript levels of murine ABCA1 gene Abca1 (Fig. 1). However, Abca1 mRNA level in the Cholesterol group did not significantly differ from that in the control group.

3.3. Effects of atherogenic diet components on mRNA expression of the FXR target genes

We further determined hepatic mRNA expression levels of FXR target genes Abcb11, Abcc2, and short heterodimer partner (SHP) [1,21], to evaluate the activation state of FXR. Both ABCB11 and ABCC2 (also known as BSEP and MRP2, respectively) are localized at the canalicular membrane of hepatocytes and excrete bile salts [21]. The nuclear receptor SHP is capable of repressing CYP7A1 expression by binding and repressing the transcriptional activity of liver receptor homolog (LRH)-1 [22,23]. As shown in Fig. 2, cholic acid with and without cholesterol + high fat (i.e., AT and CA diets) significantly increased all of these mRNA levels while cholesterol or AT – CA diet did not.

It has been shown that ABCC2 gene expression is positively regulated also by another nuclear receptor pregnane X receptor (PXR, also known as SXR) [21]. Because lithocholic acid has been identified as a ligand of PXR [24], we also determined the mRNA expression of another PXR tar-

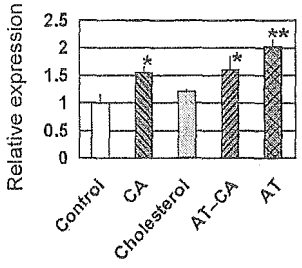

Fig. 1. Effects of atherogenic diet components on hepatic mRNA expression levels of Abca1 in mice. Male C57BL/6 mice were fed each diet for 2 weeks and thereafter, mRNA expression levels of Abca1 in the whole-liver were determined by the real-time quantitative RT-PCR. Data are mean + S.E. of 4 mice in each group and expressed as relative values to control. * $P<0.05$, ** $P<0.01$ vs. control.

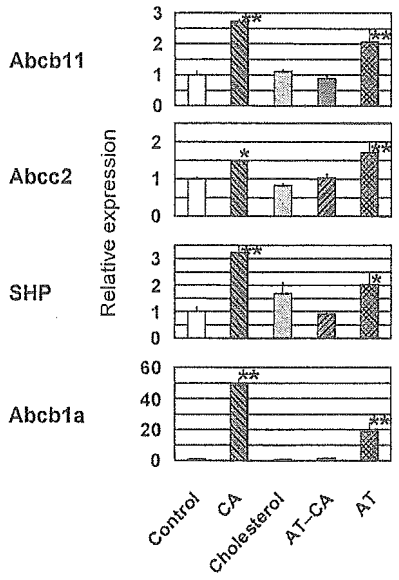

Fig. 2. Effects of atherogenic diet components on hepatic mRNA expression levels of Abcb11, Abcc2, SHP, and Abcb1a in mice. Data are mean + S.E. of 4 mice in each group (same samples shown in Fig. 1) and expressed as relative values to control. $^{*}P<0.05$, $^{**}P<0.01$ vs. control.

get gene Abcb1a/mdr1a [1,21]. Consistent with the effects on Abcc2 transcript levels, CA or AT diet significantly increased Abcb1a levels (Fig. 2). These results suggest that feeding cholic acid induces both FXR and PXR activation.

3.4. Effects of atherogenic diet components on mRNA expression of CYP7A1

Fig. 3 shows hepatic mRNA levels of CYP7A1 on each of five diets. AT − CA diet did not increase the CYP7A1 transcript level while the treatment induced the significant increase of Abca1 mRNA level (Fig. 1). Moreover, in CA and AT groups, CYP7A1 mRNA expression was greatly suppressed although LXRα might be activated. These results suggest that CYP7A1 mRNA expression is not affected by mild activation of LXRα and that FXR is the dominant regulator of CYP7A1 transcription in mice fed the atherogenic diet.

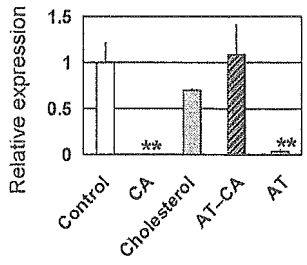

Fig. 3. Effects of atherogenic diet components on hepatic mRNA expression levels of CYP7A1 in mice. Data are mean + S.E. of 4 mice in each group (same samples shown in Fig. 1) and expressed as relative values to control. $^{**}P<0.01$ vs. control.

4. Discussion

Recently, the roles of LXRα and FXR in the regulation of CYP7A1 were evaluated in animals fed cholesterol with or without cholic acid. In the cholesterol-fed New Zealand white rabbits, both LXRα and FXR were activated, and the effect of FXR on the CYP7A1 mRNA expression overrode the effect of LXRα [11]. On the other hand, in the Sprague–Dawley rats fed cholesterol and cholic acid the effects of LXRα overrode the effects of FXR, which resulted in the induction of CYP7A1 mRNA levels [10]. However, Xu et al. [14] reported that feeding cholesterol alone did not activate FXR in Sprague–Dawley rats. In addition, they showed that feeding cholesterol with cholic acid significantly decreased CYP7A1 mRNA levels. Thus, the results in rats remain controversial, and the effect of dietary cholesterol on CYP7A1 activity seems to differ between the species.

In mice, whereas atherosclerosis and hepatic lipid metabolism has been widely studied, little is known about the effects of dietary cholesterol, high fat, or cholic acid on LXRα and FXR activation. This study demonstrated for the first time that feeding cholesterol with or without high fat to C57BL/6 mice does not affect CYP7A1 transcript levels although feeding cholesterol with high fat activates LXRα, but not FXR. Moreover, it is indicated that the inhibitory effect of FXR overrides the stimulatory effect of LXRα to suppress CYP7A1 mRNA expression in the atherogenic diet-fed mice. The effect of dietary cholesterol on CYP7A1 mRNA expression was different from those in rats and rabbits. Thus, it appears that CYP7A1 transcription is not easily activated by LXRα in the mice.

As shown in Fig. 2, feeding cholic acid to mice might induce not only FXR but PXR activation. Although PXR might play a role in the down-regulation of CYP7A1 [24], feeding cholic acid did not reduce CYP7A1 mRNA levels in FXR knock-out mice [25]. Therefore, at least in mice, CYP7A1 mRNA expression seems to be suppressed mainly via the FXR-mediated pathway. While activated FXR is thought to repress CYP7A1 through an FXR-SHP-LRH-1 cascade, feeding cholic acid to SHP knock-out mice could still inhibit CYP7A1 expression [26,27]. Additionally, in primary cultures of human hepatocytes, LXRα activation had the opposite effect, repressing CYP7A1 expression, through the induction of SHP [28]. Thus, molecular mechanisms to regulate CYP7A1 expression appear to differ between the species and remains to be clarified.

Feeding cholic acid to mice significantly increased serum LDL + VLDL cholesterol and hepatic cholesterol, and decreased serum triglyceride concentrations (Table 1). The treatment did not affect transcript levels of sterol regulatory genes, 3-hydroxy-3-methylglutaryl coenzyme A synthase 1 and LDL receptor genes (data not shown), suggesting that hepatic cholesterol synthesis was not activated in the mice fed CA or AT diet. Because CYP7A1 activity generally changes in parallel with its mRNA levels [3–5,7,8,11,14], it seems that the increase in hepatic cholesterol was greatly affected by the

suppression of CYP7A1 activity. In concordance with data shown in this study, bile acids and FXR agonists reduce serum triglyceride concentrations [1,29]. Kast et al. [29] reported that both apolipoprotein C-II and phospholipids transfer protein were induced by FXR activation and that the induction of these genes by feeding cholic acid correlated with decreased circulating triglyceride concentrations in mice. FXR agonists were also shown to induce mRNA levels of peroxisome proliferator-activated receptor α in human hepatic cells, but not in murine liver [30].

In summary, our data suggest that in mice, cholic acid component is needed for FXR activation and that both cholic acid and cholesterol + high fat are necessary for activating LXRα to a large extent. The difference of activation states of LXRα and FXR between the species must be taken into consideration when atherosclerosis in the animal models is studied.

References

[1] Chiang JY. Bile acid regulation of gene expression: roles of nuclear hormone receptors. Endocr Rev 2002;23:443–63.

[2] Jelinek DF, Andersson S, Slaughter CA, Russell DW. Cloning and regulation of cholesterol 7 alpha-hydroxylase, the rate-limiting enzyme in bile acid biosynthesis. J Biol Chem 1990;265:8190–7.

[3] Pandak WM, Li YC, Chiang JY, et al. Regulation of cholesterol 7 alpha-hydroxylase mRNA and transcriptional activity by taurocholate and cholesterol in the chronic biliary diverted rat. J Biol Chem 1991;266:3416–21.

[4] Shefer S, Nguyen LB, Sal en G, et al. Differing effects of cholesterol and taurocholate on steady state hepatic HMG-CoA reductase and cholesterol 7 alpha-hydroxylase activities and mRNA levels in the rat. J Lipid Res 1992;33:1193–200.

[5] Spady DK, Cuthbert JA. Regulation of hepatic sterol metabolism in the rat. Parallel regulation of activity and mRNA for 7 alpha-hydroxylase but not 3-hydroxy-3-methylglutaryl-coenzyme. A reductase or low density lipoprotein receptor. J Biol Chem 1992;267:5584–91.

[6] Rudel L, Deckelman C, Wilson M, Scobey M, Anderson R. Dietary cholesterol and downregulation of cholesterol 7 alpha-hydroxylase and cholesterol absorption in African green monkeys. J Clin Invest 1994;93:2463–3472.

[7] Horton JD, Cuthbert JA, Spady DK. Regulation of hepatic 7 alpha-hydroxylase expression and response to dietary cholesterol in the rat and hamster. J Biol Chem 1995;270:5381–7.

[8] Xu G, Salen G, Shefer S, et al. Unexpected inhibition of cholesterol 7 alpha-hydroxylase by cholesterol in New Zealand white and Watanabe heritable hyperlipidemic rabbits. J Clin Invest 1995;95:1497–504.

[9] Nguyen LB, Xu G, Shefer S, et al. Comparative regulation of hepatic sterol 27-hydroxylase and cholesterol 7alpha-hydroxylase activities in the rat, guinea pig, and rabbit: effects of cholesterol and bile acids. Metabolism 1999;48:1542–8.

[10] Gupta S, Pandak WM, Hylemon PB. LXR alpha is the dominant regulator of CYP7A1 transcription. Biochem Biophys Res Commun 2002;293:338–43.

[11] Xu G, Li H, Pan LX, Shang Q, Honda A, Ananthanarayanan M. FXR-mediated down-regulation of CYP7A1 dominates LXRalpha in long-term cholesterol-fed NZW rabbits. J Lipid Res 2003;44:1956–62.

[12] Roberts A, Thompson JS. Genetic factors in the development of atheroma and on serum total cholesterol levels in inbred mice and their hybrids. Prog Biochem Pharmacol 1977;13:298–305.

[13] Paigen B, Morrow A, Brandon C, Mitchell D, Holmes P. Variation in susceptibility to atherosclerosis among inbred strains of mice. Atherosclerosis 1985;57:65–73.

[14] Xu G, Pan LX, Li H, et al. Dietary cholesterol stimulates CYP7A1 in rats because farnesoid X receptor is not activated. Am J Physiol Gastrointest Liver Physiol 2004;286:G730–5.

[15] Ishibashi S, Herz J, Maeda N, Goldstein JL, Brown MS. The two-receptor model of lipoprotein clearance: tests of the hypothesis in 'knockout' mice lacking the low density lipoprotein receptor, apolipoprotein E, or both proteins. Proc Natl Acad Sci USA 1994;91:4431–5.

[16] Horton JD, Bashmakov Y, Shimomura I, Shimano H. Regulation of sterol regulatory element binding proteins in livers of fasted and refed mice. Proc Natl Acad Sci USA 1998;95:5987–92.

[17] Carr TP, Andresen CJ, Rudel LL. Enzymatic determination of triglyceride, free cholesterol, and total cholesterol in tissue lipid extracts. Clin Biochem 1993;26:39–42.

[18] Ando H, Tsuruoka S, Yamamoto H, et al. Effects of pravastatin on the expression of ATP-binding cassette transporter A1. J Pharmacol Exp Ther 2004;311:420–5.

[19] Su YR, Linton MF, Fazio S. Rapid quantification of murine ABC mRNAs by real time reverse transcriptase-polymerase chain reaction. J Lipid Res 2002;43:2180–7.

[20] Wang N, Tall AR. Regulation and mechanisms of ATP-binding cassette transporter A1-mediated cellular cholesterol efflux. Arterioscler Thromb Vasc Biol 2003;23:1178–84.

[21] Trauner M, Boyer JL. Bile salt transporters: molecular characterization, function, and regulation. Physiol Rev 2003;83:633–71.

[22] Goodwin B, Jones SA, Price RR, et al. A regulatory cascade of the nuclear receptors FXR, SHP-1, and LRH-1 represses bile acid biosynthesis. Mol Cell 2000;6:517–26.

[23] Lu TT, Makishima M, Repa JJ, et al. Molecular basis for feedback regulation of bile acid synthesis by nuclear receptors. Mol Cell 2000;6:507–15.

[24] Staudinger JL, Goodwin B, Jones SA, et al. The nuclear receptor PXR is a lithocholic acid sensor that protects against liver toxicity. Proc Natl Acad Sci USA 2001;98:3369–74.

[25] Sinal CJ, Tohkin M, Miyata M, et al. Targeted disruption of the nuclear receptor FXR/BAR impairs bile acid and lipid homeostasis. Cell 2000:731–44.

[26] Kerr TA, Saeki S, Schneider M, et al. Loss of nuclear receptor SHP impairs but does not eliminate negative feedback regulation of bile acid synthesis. Dev Cell 2002;2:713–20.

[27] Wang L, Lee YK, Bundman D, et al. Redundant pathways for negative feedback regulation of bile acid production. Dev Cell 2002;2:721–31.

[28] Goodwin B, Watson MA, Kim H, et al. Differential regulation of rat and human CYP7A1 by the nuclear oxysterol receptor liver X receptor-alpha. Mol Endocrinol 2003;17:386–94.

[29] Kast HR, Nguyen CM, Sinal CJ, et al. Farnesoid X-activated receptor induces apolipoprotein C-II transcription: a molecular mechanism linking plasma triglyceride levels to bile acids. Mol Endocrinol 2001;15:1720–8.

[30] Torra IP, Claudel T, Duval C, et al. Bile acids induce the expression of the human peroxisome proliferator-activated receptor alpha gene via activation of the farnesoid X receptor. Mol Endocrinol 2003;17:259–72.

Original Report: Laboratory Investigation

American Journal of Nephrology

Am J Nephrol 2005;25:233–239
DOI: 10.1159/000085969

Received: January 27, 2005
Accepted: April 20, 2005
Published online: May 24, 2005

Citrate Reverses Cyclosporin A-Induced Metabolic Acidosis and Bone Resorption in Rats

Shuichi Tsuruoka[a] George J. Schwartz[b] Takashi Ioka[a] Hisashi Yamamoto[a] Hitoshi Ando[a] Akio Fujimura[a]

[a]Department of Pharmacology, Division of Clinical Pharmacology, Jichi Medical School, Tochigi, Japan, and [b]Department of Pediatrics, Division of Nephrology, University of Rochester School of Medicine and Dentistry, Rochester, N.Y., USA

Key Words

Cyclosporine A · Renal tubular acidosis · Alkali supplementation · Collecting duct · Osteoporosis · Nitric oxide

Abstract

Background: Cyclosporine A (CsA) causes distal renal tubular acidosis (RTA) and osteoporosis. We have recently reported that the reduction of nitric oxide (NO) exacerbates this condition. Distal RTA may deplete bone mineral due to the chronic buffering of acid in the blood. The interaction of CsA and NO in causing metabolic acidosis and bone demineralization has not been studied previously. Nor has the salubrious effect of citrate therapy. ***Purpose:*** To examine the effect of systemic pH correction by citrate on renal electrolyte (Na, K, Cl, NH_3, HCO_3) excretion following acute water loading in CsA-treated and NO-reduced rats. We further evaluated femoral bone density and bone demineralization activity after the same treatments. ***Methods:*** Rats received CsA, *L*-arginine (*L*-Arg), or nitro-*L*-arginine-methyl ester (*L*-NAME), or a combination of CsA+*L*-NAME plus or minus citrate. Urine and blood electrolytes were examined, as well as the urine excretion of deoxypyridinoline and the bone density of both femurs. ***Results:*** CsA and *L*-NAME reduced urine pH and the serum HCO_3^- concentration, and increased serum K^+ and Cl^- concentrations. The combination of CsA with *L*-NAME caused more severe deficits in the serum HCO_3^- concentration and elevations in serum K^+ and Cl^- concentrations than either drug alone. Both CsA and *L*-NAME reduced urinary nitrate excretion, which was reversed by co-administration of *L*-Arg. Co-administration of citrate or *L*-Arg improved the CsA- and *L*-NAME-induced acidosis and hyperkalemia. Bone resorption and density of the femurs were decreased by CsA and *L*-NAME and were additive for both drugs. Co-administration of citrate or *L*-Arg restored both bone resorption and density to normal levels. ***Conclusion:*** CsA induces a hyperchloremic metabolic acidosis with hyperkalemia and a reduction in NO. The ensuing systemic acidosis causes bone resorption and demineralization. These effects were corrected by co-treatment with citrate. Citrate, at least in part, directly reduces the protonation of bone in animals treated with CsA and is recommended as a potential adjunct drug to prevent bone demineralization in patients chronically receiving CsA.

KARGER

Fax +41 61 306 12 34
E-Mail karger@karger.ch
www.karger.com

Accessible online at:
www.karger.com/ajn

Shuichi Tsuruoka, MD
Department of Pharmacology, Division of Clinical Pharmacology
Jichi Medical School, 3311 Yakushiji, Mimamikawachi
Kawachi, Tochigi 329-0498 (Japan)
Tel. +81 285 58 7388, Fax +81 285 44 7562, E-Mail tsuru@jichi.ac.jp

Introduction

Cyclosporine A (CsA) is widely used as an immunosuppressive agent for the treatment of various diseases. It is well recognized that CsA causes nephropathy, which is mainly due to the vasoconstriction of the renal artery by a reduction in nitric oxide (NO) production [1, 2]. It is also reported that CsA causes distal renal tubular acidosis (RTA) [3–6], and this is important because systemic acidosis may limit skeletal and organ growth. We have recently reported that the CsA-induced distal RTA is likely mediated by a reduction in NO production [7].

In addition, CsA causes osteoporosis in both humans [8] and rats [9]. Fiore et al. [9] reported that CsA-induced osteoporosis was prevented by the addition of *L*-arginine (*L*-Arg), a substrate of NO synthase, in rats. On the other hand, proton secretion in osteoclasts is regulated by NO [10], and this effect is believed to be independent of systemic pH. From these data and because bone is one of the major buffers of acid in the blood, we would suggest that treatment of CsA-induced RTA by the NO donor *L*-Arg would reduce bone resorption. We hypothesize that correction of systemic pH without restoring NO would alleviate the bone demineralization due to CsA.

To test the above hypothesis and understand the mechanisms of the CsA-induced acid-base disturbance in more detail, we examined the effect on bone of correcting acidosis by administering *L*-Arg or citrate to rats receiving CsA and/or nitro-*L*-arginine-methyl ester (*L*-NAME), an inhibitor of NO synthase.

Methods

Animals and Treatments

Male Wistar rats (8 weeks old, n = 96) were used in this study. They were maintained in a specific pathogen-free room with free access to standard rat chow (CE-2, Japan Clea Co, Ltd., containing Na 0.3 g/100 g, K 1.06 g/100 g, Ca 1.18 g/100 g) and distilled water. Temperature and humidity were automatically controlled in the room. All the experiments were conducted in accordance with the Jichi Medical School Guidelines for Laboratory Animals.

CsA (7.5 mg/kg) [7, 11] or vehicle (olive oil) was given to rats by nasogastric tube once a day in the morning for 6 weeks. *L*-NAME (12.5 mg/kg for low dose and 30 mg/kg for high dose), *L*-Arg (8.5 mg/kg) [11], calcium citrate monohydrate (5 mmol/kg for low dose and 10 mmol/kg for high dose) [12], or vehicle (distilled water) were also given to these animals twice daily (every 12 h) for 6 weeks by nasogastric tube. Each agent was diluted in distilled water.

The animals were randomly divided into 12 groups as follows: vehicle (n = 10); CsA (n = 10); CsA+citrate (low, n = 7); CsA+citrate (high, n = 10); CsA+*L*-Arg (n = 8); *L*-Arg (n = 9); *L*-NAME (low, n = 8); *L*-NAME (high, n = 8); *L*-NAME (high)+citrate (high, n = 10); CsA+*L*-NAME (low, n = 10); CsA+*L*-NAME (low)+citrate (low, n = 8), and CsA+*L*-NAME (low)+citrate (high, n = 8).

The dosages of *L*-NAME and *L*-Arg were determined empirically to be those that minimally inhibited weight gain. Because preliminary studies showed that the body weight in the CsA+*L*-NAME (high dose) group was significantly decreased, and the reduction itself might affect acid-base status in these animals, we selected a lower dose of *L*-NAME for the combination treatment of *L*-NAME+CsA or *L*-NAME+CsA+citrate [7].

Systolic arterial blood pressure was measured by a tail-cuff method on a weekly basis. The dose of CsA (7.5 mg/kg) has previously been shown not to elevate blood pressure in rats [7, 11].

Water-Loaded Clearance Studies

Water-loaded clearances were performed 6 weeks after initiation of the study [7]. On the day of each test, animals were weighed and then received distilled water, 3% of body weight, by nasogastric tube. Thereafter, each animal was placed in a metabolic cage for a 4-hour urine collection under water-saturated light mineral oil to avoid evaporation [13, 14]. Urine volumes were measured. After the end of the urine collection, the animals were placed in a small cage to avoid movement during the blood sampling.

Approximately 3 ml of blood was obtained from the tail vein by insertion of a 22-gauge needle. Part of the blood was mixed with approximately 0.05 ml of heparin for measurement of the bicarbonate concentration, and the rest was allowed to clot and was centrifuged to provide a serum sample. Urine pH was measured immediately after the end of the collection. A portion of the collected urine was added with a mixture of sulfonic acid/sodium tungstate to remove protein and used for measurement of NH_3. The rest was kept frozen until the measurement of electrolytes and NO.

Assay Methods

Urine pH, and concentrations of creatinine, Na, K, and Cl in serum and urine were measured by an electrometer (HM-16S, Toa electronics, Japan) and autoanalyzer (Hitachi 716S), respectively. The bicarbonate concentration was determined by an enzymatic method (Sigma diagnostic kit, 132-A). The ammonia concentration was measured by the Berthelot reaction [15]. The urinary nitrate and nitrite concentrations (NO_2+NO_3), stable metabolites of NO in the urine, were determined by colorimetric assay (Nitrate/Nitrite colorimetric assay kit, Cayman Chemicals, Ann Arbor, Mich., USA) [7]. Urine excretion of bicarbonate and ammonia were calculated from urine concentration × urine flow rate and expressed as micromoles per 4 h. Urine metabolites of NO (nitrate and nitrite) were expressed as nanomoles per microgram creatinine.

Urine deoxypyridinoline (DPD), an index of bone resorption, was measured by a reverse-phase HPLC [16] and its excretion was expressed as a ratio to the creatinine concentration in picomoles per micromole [14, 17, 18]. The bone density of both femurs was determined by dual energy X-ray absorption (DCS-600A, Aloka, Japan) [14, 18]. The scan was performed every 2 mm along the axis of the bone from the proximal end. Usually 14–17 scans were done in each bone and the data were averaged [19].

Statistics

All data are presented as the mean ± SE. Statistical analysis was performed by one-way analysis of variance (ANOVA) and the Fisher's Protected Least Significant Difference (PLSD) test was

used to compare the groups as a post-hoc test. These analyses were done using StatView 5 for Windows (SAS Institute Inc., Cary, N.C., USA). $p < 0.05$ was regarded as significant.

Results

Glomerular Filtration Rate and Systolic Blood Pressure

All animals completed the study without any significant body weight loss.

In order to validate our 4-hour creatinine clearance test following water challenge, we conducted simultaneous inulin clearances in 3 normal and 3 hemi-nephrectomized rats [20]. The creatinine clearance was not statistically different from the inulin clearance in both normal and hemi-nephrectomized rats (6.06 ± 0.28 and 3.76 ± 0.17 ml/min/kg body weight for creatinine clearance and 6.23 ± 0.25 and 3.67 ± 0.35 ml/min/kg for inulin clearance in normal and hemi-nephrectomized rats, respectively; $p > 0.1$ in both groups).

Creatinine clearance during the distilled water challenge test was not different among any treatments (table 1). Systolic blood pressure 1 day prior to water loading and body weight on the day of the clearance study were not different among any treatments (table 1).

Urine pH, Serum Electrolytes and Urinary Excretion

Urine pH after water loading was reduced by CsA and *L*-NAME, and was ameliorated by co-administration of citrate or *L*-Arg (table 2). The CsA-induced reduction in urine pH was further reduced by co-administration of *L*-NAME, while it was ameliorated by co-administration of *L*-Arg. The CsA- and *L*-NAME-induced reduction in urine pH was also improved by co-administration of citrate in a dose-dependent manner. *L*-Arg alone did not affect the urine pH.

The serum bicarbonate concentration after water loading was decreased by treatment with CsA and *L*-NAME (table 3). This suppressive effect was additive for CsA and *L*-NAME. Decreased serum bicarbonate was improved by co-administration of *L*-Arg or citrate, the latter in a dose-dependent manner.

Serum K and Cl after water loading were increased by the treatment with CsA and/or *L*-NAME (table 3). They were reduced by co-administration of *L*-Arg or citrate. Urine bicarbonate excretion after challenge of distilled water was almost negligible in all groups, but it was markedly increased by co-administration of citrate to animals treated with CsA and/or *L*-NAME (table 2). Urine NH_3 excretion was not altered by these treatments and averaged approximately 20–30 μg/4 h (data not shown).

Table 1. Creatinine clearance (Ccr) and systolic blood pressure (SBP)

	Ccr ml/min/kg	SBP mm Hg	Body weight, g
Vehicle	6.0 ± 0.3	112 ± 4	301 ± 7
CsA	5.8 ± 0.5	110 ± 3	295 ± 9
CsA+citrate (low)	5.9 ± 0.5	113 ± 4	298 ± 10
CsA+citrate (high)	5.5 ± 0.4,	111 ± 4	299 ± 9
CsA+*L*-Arg	5.6 ± 0.6	113 ± 5	297 ± 10
L-Arg	5.7 ± 0.6	111 ± 5	302 ± 9
L-NAME (low)	5.9 ± 0.5	112 ± 5	296 ± 12
L-NAME (high)	5.8 ± 0.5	110 ± 4	298 ± 10
L-NAME (high)+citrate (high)	5.5 ± 0.4	109 ± 5	296 ± 11
CsA+*L*-NAME (low)	5.7 ± 0.5	110 ± 5	295 ± 12
CsA+*L*-NAME (low)+citrate (low)	5.9 ± 0.5	111 ± 5	297 ± 11
CsA+*L*-NAME (low)+citrate (high)	6.0 ± 0.5	113 ± 5	301 ± 11

No significant differences in Ccr, SBP or body weight were detected among the groups using Fisher's protected least significant difference test. Body weight was measured just before Ccr measurement.

Table 2. Urine pH and bicarbonate excretion after acute loading of distilled water to rats

	Urine pH	Urine HCO_3 μmol/4 h
Vehicle	7.26 ± 0.10[b, c]	9.7 ± 5.1
CsA	6.89 ± 0.11[a]	12.7 ± 4.8
CsA+citrate (low)	7.38 ± 0.16[b, c]	13.8 ± 5.7
CsA+citrate (high)	7.48 ± 0.13[b, c]	67.2 ± 29[a–c]
CsA+*L*-Arg	7.24 ± 0.14[b, c]	13.5 ± 7
L-Arg	7.29 ± 0.16[b, c]	15.2 ± 7.9
L-NAME (low)	7.31 ± 0.14[b, c]	15.7 ± 8
L-NAME (high)	6.85 ± 0.15[a]	14.8 ± 6.8
L-NAME (high)+citrate (high)	7.3 ± 0.14[b, c]	45 ± 19[a–c]
CsA+*L*-NAME (low)	6.76 ± 0.13[a]	13.1 ± 6.9
CsA+*L*-NAME (low)+citrate (low)	6.89 ± 0.14[a]	14.9 ± 7.9
CsA+*L*-NAME (low)+citrate (high)	7.35 ± 0.16[b, c]	28.8 ± 9.8[a–c]

Free voided urine was collected for 4 h in a metabolic cage just after the water loading. Blood was obtained from the tail vein just after the end of the collection of urine. Animals were treated for 6 weeks. Water loading was conducted 6 weeks after starting treatment. n = 10 in each group except for CsA+*L*-Arg (n = 8), CsA+*L*-NAME+citrate (low, n = 8), CsA+*L*-NAME+citrate (high, n = 8), and *L*-Arg (n = 9).

[a] $p < 0.05$ vs. vehicle.

[b] $p < 0.05$ vs. CsA.

[c] $p < 0.05$ vs. CsA+*L*-NAME (low).

Table 3. Serum concentrations of bicarbonate, potassium and chloride after acute loading of distilled water to rats

	HCO_3, m*M*	K, m*M*	Cl, m*M*
Vehicle	$24.2 \pm 0.2^{b,c}$	$3.62 \pm 0.07^{b,c}$	$107.5 \pm 1.3^{b,c}$
CsA	$21.8 \pm 1.0^{a,c}$	4.51 ± 0.16^{a}	$112.5 \pm 1.2^{a,c}$
CsA+citrate (low)	22.7 ± 0.9	$3.62 \pm 0.10^{b,c}$	$107.8 \pm 1.7^{b,c}$
CsA+citrate (high)	$24.7 \pm 1.0^{b,c}$	$3.62 \pm 0.09^{b,c}$	$105.3 \pm 1.8^{b,c}$
CsA+*L*-Arg	$23.9 \pm 1.3^{b,c}$	$3.68 \pm 0.16^{b,c}$	110.8 ± 1.6^{c}
L-Arg	$24.4 \pm 0.9^{b,c}$	$3.67 \pm 0.11^{b,c}$	$109.5 \pm 1.5^{b,c}$
L-NAME (low)	$24.2 \pm 0.8^{b,c}$	$3.68 \pm 0.10^{b,c}$	$108.5 \pm 1.9^{b,c}$
L-NAME (high)	21.2 ± 1.2^{a}	4.42 ± 0.17^{a}	114.2 ± 2.1^{a}
L-NAME (high)+citrate (high)	$23.9 \pm 1.0^{b,c}$	$3.88 \pm 0.13^{b,c}$	$109.5 \pm 1.7^{b,c}$
CsA+*L*-NAME (low)	$19.2 \pm 1.5^{a,b}$	4.65 ± 0.15^{a}	$117.9 \pm 1.5^{a,b}$
CsA+*L*-NAME (low)+citrate (low)	21.1 ± 1.3^{a}	4.38 ± 0.13^{a}	114.2 ± 2.1^{a}
CsA+*L*-NAME (low)+citrate (high)	$25.9 \pm 1.1^{b,c}$	$3.75 \pm 0.14^{b,c}$	$107.4 \pm 1.4^{b,c}$

Free voided urine was collected for 4 h in a metabolic cage just after water loading. Blood was obtained from the tail vein just after the end of the collection of urine. Animals were treated for 6 weeks. Water loading was conducted 6 weeks after starting treatment. n = 10 in each group except for CsA+*L*-Arg (n = 8), CsA+*L*-NAME+citrate (low, n = 8), CsA+*L*-NAME+citrate (high, n = 8), and *L*-Arg (n = 9).

[a] $p < 0.05$ vs. vehicle.

[b] $p < 0.05$ vs. CsA.

[c] $p < 0.05$ vs. CsA+*L*-NAME (low).

Bone Resorption and Density

To evaluate the contribution of buffering by bone during the treatments, we measured the urinary excretion of DPD, a marker of bone resorption following water loading (table 4). DPD excretion was increased by CsA, *L*-NAME, and their combination. This increase in DPD excretion was partially attenuated by co-administration of *L*-Arg or low-dose citrate and completely reversed by high-dose citrate. We also measured the bone density of the femur after water loading. It was decreased by CsA and *L*-NAME and their combination, but the decrease was attenuated by co-administration of *L*-Arg or citrate (table 4). The effects were comparable in proximal, medial, and distal femurs (data not shown).

Urinary Nitrate/Nitrite Excretion

The urinary nitrate concentration was decreased in animals treated with CsA+*L*-NAME and *L*-NAME, which is compatible with our recent report [7]. *L*-Arg with or without CsA caused an increase in urinary nitrate/nitrite excretion compared to vehicle or CsA (fig. 1). As expected, *L*-NAME, alone or in combination, reduced urinary nitrate/nitrite excretion, and this reduction was not reversed to normal levels by co-administration of citrate.

Table 4. Urine deoxypyridinoline (DPD) excretion and bone density of the femur at the end of the study

	DPD pmol/μmol Cr	Bone density mg/cm^2
Vehicle	$57 \pm 4^{b,c}$	$170 \pm 7^{b,c}$
CsA	$117 \pm 9^{a,c}$	$120 \pm 12^{a,c}$
CsA+citrate (low)	110 ± 13^{a}	131 ± 16^{a}
CsA+citrate (high)	$78 \pm 10^{b,c}$	$163 \pm 13^{b,c}$
CsA+*L*-Arg	$87 \pm 12^{a,b}$	148 ± 21
L-Arg	$57 \pm 6^{b,c}$	$172 \pm 13^{b,c}$
L-NAME (low)	$58 \pm 6^{b,c}$	$168 \pm 14^{b,c}$
L-NAME (high)	$102 \pm 11^{a,c}$	129 ± 16^{a}
L-NAME (high)+citrate (high)	$66 \pm 12^{b,c}$	$159 \pm 15^{b,c}$
CsA+*L*-NAME (low)	$154 \pm 13^{a,b}$	$90 \pm 13^{a,c}$
CsA+*L*-NAME (low)+citrate (low)	$152 \pm 7^{a,b}$	112 ± 14^{a}
CsA+*L*-NAME (low)+citrate (high)	$80 \pm 6^{b,c}$	$154 \pm 11^{b,c}$

Animals were treated for 6 weeks. Free voided urine was collected for 4 h in a metabolic cage just after water loading.

The bone density scan was performed every 2 mm along with the axis of the bone from the proximal end. Overall averaging of the first proximal 3 scans, middle 4 scans, and last 3 scans (regarded as 'proximal', 'medial' and 'distal', respectively) provided the determination of bone density in milligrams per square centimeter. 'Medial' is exclusively cortical bone and 'distal' is rich in cancellous bone.

[a] $p < 0.05$ vs. vehicle.

[b] $p < 0.05$ vs. CsA.

[c] $p < 0.05$ vs. CsA+*L*-NAME (low).

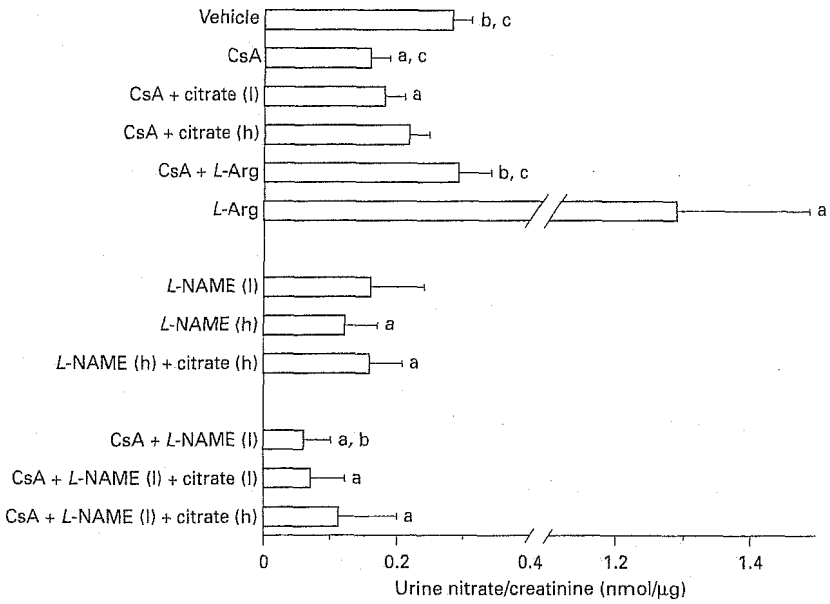

Fig. 1. Urine excretion of nitric oxide measured as nitrate and nitrite metabolites (nmol/μg creatinine) after an acute loading of distilled water to rats. Animals were treated for 6 weeks. Free voided urine was collected for 4 h in a metabolic cage just after water loading. l = Low dose; h = high dose. [a] $p < 0.05$ vs. vehicle; [b] $p < 0.05$ vs. CsA; [c] $p < 0.05$ vs. CsA+*L*-NAME (low).

Discussion

We have recently reported that the administration of CsA leads to hyperkalemic distal RTA, and a reduction in NO possibly mediates the effect of CsA [7]. Because bone tissue is one of the major buffers of acid in the body, treatment of reduced NO production by *L*-Arg may indirectly improve bone composition. In addition, correction of systemic pH potentially attenuates the bone disorder induced by CsA. To address the issue, we examined the effect of citrate and found that the demineralization caused by CsA and by NO inhibition (*L*-NAME) were both corrected by citrate, as was the reduced serum bicarbonate level. Although we did not evaluate the effect of acute acid loading in this study, every abnormal serum/urine value was corrected by the co-administration of citrate. To our knowledge, this is the first study to treat CsA-induced osteoporosis by the augmentation of systemic pH with citrate.

Our results, which showed the additive effects of CsA and NO inhibition, are somewhat indirect, relying on bone density measurements, urine excretion of NO metabolites, and urine markers of bone resorption. Further studies are required to dissect and understand the relationship between systemic and local effects on bone demineralization; that is, on osteoclast function, NO expression, and pH. Nevertheless, the additive effects of CsA and NO inhibition were very intriguing, suggesting the possibility of different pathways causing acidosis and bone resorption.

Osteoclast activity was decreased by providing NO through *L*-Arg (table 4), as well as by correcting acidosis with citrate in this study. It is possible that osteoclast activity is stimulated by a reduction in NO [21], although citrate did not elevate urinary nitrate/nitrite (fig. 1), an effect that would have been expected to reduce osteoclast activity. Citrate as well as *L*-Arg improved the effect of CsA and/or *L*-NAME on bone. Serum bicarbonate concentration during water loading was reduced in the CsA+*L*-NAME group compared with the vehicle group. Under these conditions urine bicarbonate excretion was increased by co-administration of citrate, suggesting a role for systemic alkalinization by citrate. Citrate, at least in part, directly affects the protonation of bone buffers in animals treated with CsA and, by being converted to bicarbonate thereby results in increased urinary bicarbonate excretion. Thus, citrate corrects the acidosis by providing potential HCO_3 (from metabolism) and this HCO_3 would reverse the bone buffering of acid. Whether or not treatment with other bases, such as $NaHCO_3$, can prevent bone demineralization is worthy of further investigation.

L-Arg has been used for the treatment of hyperammonemia in patients with congenital disorders of the urea cycle. *L*-Arg restored to normal the reduced levels of bicarbonate, in the serum of CsA- and *L*-NAME-treated rats. However, it is known that *L*-Arg is not substantially metabolized to bicarbonate. Whether or not *L*-Arg can prevent bone demineralization in patients treated long-term with CsA remains to be determined. The relationship between CsA, bone demineralization, decreased NO, and correction of pH by citrate should be further investigated using in vitro studies in osteoclasts and bone slices.

It is known that a high-dose of *L*-NAME reduces the glomerular filtration rate due to constriction of the afferent arteriole [22] and this may indirectly affect the acid-base status. However, as we showed in this and in previous studies, *L*-NAME at the dose used in this study did not affect creatinine clearance, blood pressure, or body weight. Therefore, we believe that the observed phenomena in this study are not due to an alteration in glomerular filtration rate.

Recently, it has been shown that decreased serum potassium directly stimulates osteoclast activity [23]. In our study the serum potassium concentration was inversely related to the urine pH and serum bicarbonate concentration. Therefore, the elevation in serum potassium by CsA and by inhibiting NO synthesis would be expected to cause decreased bone resorption. However, in association with the higher serum potassium concentration, in the CsA and *L*-NAME groups we found increased DPD excretion and decreased bone density. Thus, the major effect of CsA and *L*-NAME to cause chronic acidosis with bone demineralization predominates over any putative potassium effect.

Our studies indicate that CsA causes demineralization of bone and a reduction in bone density, in part by causing chronic acidosis, and the resulting acidosis leads to the protonation and demineralization of bone. The administration of citrate prevents CsA-induced bone demineralization and might be recommended for patients on long-term CsA treatment. Citrate is readily available as sodium or potassium citrate, the latter of which is used to prevent kidney stones in patients with urinary calcium supersaturation. Future studies to measure bone buffering and net bicarbonate transport in rat collecting ducts after citrate plus CsA treatment would be helpful to further investigate the potential merits of this therapy.

In conclusion, we reported that CsA-induced distal RTA was corrected by supplementation of citrate in rats. The distal RTA caused by the CsA was corrected in parallel with the correction of CsA-induced osteoporosis. Citrate, at least in part, directly reduces the protonation of bone in animals treated with CsA and should be considered as adjunct therapy for patients chronically receiving CsA.

Acknowledgements

This study was partly supported by a grant from the Ministry of Education, Culture, Sports, Science and Technology of Japan (to S.T.). G.J.S was supported in part by USPHS NIH grant No. DK-50603.

References

1 Bennet W: Cyclosporine nephrotoxicity. Ann Intern Med 1983;99:851–854.
2 Bennet W, DeMattos A, Meyer M, Andoh T, Barry J: Chronic cyclosporine nephropathy; the Achilles' heel of immunosupressive therapy. Kidney Int 1996;50:1089–1110.
3 Batlle D, Gutterman C, Tarka J, Prasad R: Effect of short-term cyclosporine A administration on urinary acidification. Clin Nephrol 1986;25(suppl 1):S62–S69.
4 Stahl R, Kanz L, Maier B, Schollmeyer P: Hyperchloremic metabolic acidosis with high serum potassium in renal transplant recipients: A cyclosporine A associated side effect. Clin Nephrol 1986;25:245–248.
5 Heering P, Degenhardt S, Grabensee B: Tubular dysfunction following kidney transplantation. Nephron 1996;74:501–511.
6 Aguilera S, Deray G, Desjobert H, Benhmida M, Le Hoang P, Jacobs C: Effects of cyclosporine on tubular acidification function in patients with idiopathic uveitis. Am J Nephrol 1992;12:425–430.
7 Tsuruoka S, Schwartz GJ, Wakaumi M, Nishiki K, Yamamoto H, Purkerson JM, Fujimura A: Nitric oxide production modulates cyclosporin A-induced distal renal tubular acidosis in the rat. J Pharmacol Exp Ther 2003;305:840–845.
8 Epstein S: Post-transplantation bone disease: The role of immunosuppressive agents and the skeleton. J Bone Miner Res 1996;11:1–7.
9 Fiore C, Pennisi P, Cutuli V, Prato A, Messina R, Clementi G: *L*-Arginine prevents bone loss and bone collagen breakdown in cyclosporin A-treated rats. Eur J Pharmacol 2000;408:323–326.
10 Van Epps-Fung C, Williams JP, Cornwell TL, Lincoln TM, McDonald JM, Radding W, Blair HC: Regulation of osteoclastic acid secretion by cGMP-dependent protein kinase. Biochem Biophys Res Commun 1994;204:565–571.
11 Shihab F, Yi H, Bennett W, Andoh T: Effect of nitric oxide modulation on TGF-beta1 and matrix proteins in chronic cyclosporine nephrotoxicity. Kidney Int 2000;58:1174–1185.
12 Domrongkitchaiporn S, Pongskul C, Sirikulchayanonta V, Stitchantrakul W, Leeprasert V, Ongphiphadhanakul B, Radinahamed P, Rajatanavin R: Bone histology and bone mineral density after correction of acidosis in distal renal tubular acidosis. Kidney Int 2002;62:2120–2126.

13 Tsuruoka S, Sugimoto K-I, Fujimura A: Contribution of diet to the dosing time-dependent change of vitamin D3-induced hypercalcemia in rats. Life Sci 2000;68:579–582.
14 Tsuruoka S, Nishiki K, Sugimoto K, Fujimura A: Chronotherapy with active vitamin D3 in aged stroke-prone spontaneously hypertensive rats. a model of osteoporosis. Eur J Pharmacol 2001;428:287–293.
15 Killeen G, Hynes M, Power R, Walsh G, Headon D: An ultrafiltration method for the removal of interfering agents and its application to the determination of free ammonia in solutions of oxystarch by the Berthelot reaction method. Anal Biochem 1993;215:284–291.
16 Seyedin S, Kung V, Danilhoff Y, Hesley R, Gomez B, Nielsen L, Rosen H, Zuk R: Immunoassay for urinary pyridinoline: The new marker of bone resorption. J.Bone Miner Metab 1993; 8:635–642.
17 Yoshitake K, Yokota K, Kasugai Y, Kagawa M, Sukamoto T, Nakamura T: Effects of 16 weeks of treatment with tibolone on bone mass and bone mechanical and histomorphometric indices in mature ovariectomized rats with established osteopenia on a low-calcium diet. Bone 1999;25:311–319.
18 Tsuruoka S, Nishiki K, Sugimoto K, Fujimura A: Time of day improves efficacy and reduces adverse reactions of vitamin D3 in 5/6 nephrectomized rat. Life Sci 2002;71:1809–1820.
19 Shen V, Birchman R, Xu R, Lindsay R, Dempster DW: Short-term changes in histomorphometric and biochemical turnover markers and bone mineral density in estrogen- and/or dietary calcium-deficient rats. Bone 1995;16: 149–156.
20 Kawaguchi A, Sugimoto K, Fujimura A: Preventive effect of platelet-activating factor antagonist, Y-24180, against cyclosporine-induced acute nephrotoxicity. Life Sci 2001;68: 1181–1190.
21 Kasten TP, Collin-Osdoby P, Patel N, Osdoby P, Krukowski M, Misko TP, Settle SL, Currie MG, Nickols GA: Potentiation of osteoclast bone-resorption activity by inhibition of nitric oxide synthase. Proc Natl Acad Sci USA 1994; 91:3569–3573.
22 Bobadilla N, Tapia E, Franco M, Lopez P, Mendoza S, Garcia-Torres R, Alvarado J, Herrera-Acosta J: Role of nitric oxide in renal hemodynamic abnormalities of cyclosporin nephrotoxicity. Kidney Int 1994;46:773–779.
23 Bushinsky D, Riordon D, Chan J, Krieger N: Decreased potassium stimulates bone resorption. Am J Physiol 1997;272:F774–F780.

British Journal of Clinical Pharmacology DOI:10.1111/j.1365-2125.2005.02394.x

Angiotensin II receptor blocker-induces blunted taste sensitivity: comparison of candesartan and valsartan

Shuichi Tsuruoka, Michi Wakaumi, Takashi Ioka, Hisashi Yamamoto, Hitoshi Ando, Kohichi Sugimoto & Akio Fujimura
Department of Pharmacology, Division of Clinical Pharmacology, Jichi Medical School, Tochigi, Japan.

Correspondence
Shuichi Tsuruoka, MD, Department of Pharmacology, Division of Clinical Pharmacology, Jichi Medical School, 3311 Yakushiji, Minamikawachi, Kawachi, Tochigi 329–0498, Japan.
Tel: +81 285 58 7388
Fax: +81 285 44 7562
E-mail: tsuru@jichi.ac.jp

Keywords
dysgeusia, angiotensin-II receptor blockers, adverse reactions, gustometry

Received
24 August 2004
Accepted
13 December 2004

Aims
To compare the degree of taste disturbance by candesartan and valsartan.

Methods
Candesartan cilexetil (4 mg day^{-1}), valsartan (40 mg day^{-1}), or vehicle was given to subjects (n = 8) for 13 days in a randomized, placebo-controlled, three-way crossover design with a 14-days washout period. Gustometry by filter-paper test and electrogustometry were performed before and at the end of each trial. Plasma renin activity and zinc concentrations in serum and saliva were measured.

Results
Detection thresholds of four basic tastes (sweet, salty, sour and bitter) by paper-disc test and electrogustometry were significantly worsened and plasma renin activity was elevated after the test, while the effects of two drugs did not significantly differ. These drugs did not affect zinc concentrations.

Conclusion
Both candesartan and valsartan similarly alter taste sensitivity after the repeated dosing of the drug.

Introduction

Taste disturbance is caused by several endogenous and exogenous factors, about 20% of which are drug-related including antihypertensive drugs [1, 2]. Angiotensin converting enzyme inhibitors are well known to cause the taste disturbances by either serum zinc concentration-dependent or -independent mechanisms [2–4]. However, information for angiotensin II receptor blocker (ARB) is limited. There are three case reports about ARB-induced taste disturbance (losartan [5, 6] and valsartan [7]). We have recently showed that the taste sensitivity was subclinically disturbed by candesartan, another ARB, in healthy subjects [8]. These findings indicate that this effect might be a class effect of ARB. However, this hypothesis is not proven, because ARB-induced taste disturbance was prospectively detected only for candesartan by our previous report, but not for other ARBs. To prove this, we need to evaluate the effect on taste of several other ARBs. In such a case, comparison with candesartan as well as placebo is preferable. In this study, we compared the effect of the repeated oral dosing of two different ARBs, candesartan

and valsartan, on taste sensitivity by a randomized, double-blind, placebo-controlled, crossover study in healthy subjects.

Methods

Eight healthy nonsmoking men (29–47 years) were enrolled in this study. All subjects gave written informed consent. The study design was a randomized, double-blind, placebo-controlled, three-way crossover design with a 2-week washout period. On Day 1 (observation period), the detection thresholds for tastes were determined and salivary fluid was obtained at 09.00 h, 12.00 h, 15.00 h and 21.00 h. Subjects took candesartan cilexetil (Blopress®, Takeda Pharmaceutical Co. Ltd, Tokyo, Japan, 4 mg), valsartan (Diovan®, Novartis, Pharma Co. Ltd, Tokyo, Japan, 40 mg) or placebo (100 mg of lactose) at 09.00 h from Day 2 to Day 14. On Day 14, the evaluation test and samplings of salivary fluid and blood were performed at 09.00 h, 12.00 h, 15.00 h and 21.00 h. On the day of taste evaluation, a similar light meal (sandwich with milk) was served for lunch to all subjects at 15.00 h. Subjects were prohibited from taking any other food or drink until the end of the test. Blood pressure at 24 h before final dosing of the drug was measured in each subject. After the washout period for 2 weeks, an identical protocol was repeated in a crossover fashion. The protocol was approved by the Ethical Committee of Jichi Medical School.

Two types of gustometries were performed in each subject [8]. (1) Semi-quantitative clinical gustometry using filter-paper discs (the filter-paper disc method: Taste disc®, Sanwa Chemical Laboratory, Nagoya, Japan) which is routinely used for the evaluation of dysgeusia in the clinical setting [9–11]. In brief, recognition thresholds for four basic tastes (sweet, salty, sour and bitter) were evaluated using the chemical solutions (sucrose, NaCl, tartaric acid and quinine, respectively). The solutions were sequentially diluted with distilled water into five grades (1 is the lowest). A droplet of each solution was added to filter paper, placed on the left side of the tongue 2 cm from the tip (i.e. locus for left chorda tympani nerve). Subjects selected a single answer from the following list: sweet, salty, sour, bitter, unidentifiable taste, or no taste. (2) Electrogustrometer, as routinely used for the evaluation of hypogeusia in oto-rhino-laryngology clinic, performed according to the method of Tomita *et al.* [9, 10, 12] using commercially available equipment (TR-06®, Rion Co., Ltd, Tokyo, Japan). In brief, a single type stimulation rod was placed on the left side of the tongue 2 cm from the tip. The smallest stimulus that the subjects noticed was regarded as the detection threshold. Normal range was less than +14 dB [9, 10, 12].

Spontaneously salivated salivary fluid was collected into a special polyethylene tube after gargling with distilled water three times [8]. Blood samples were taken from the cubital vein. Both salivary fluid and serum/plasma were stored at –80°C until the assay. Total zinc concentration was measured by atomic absorption spectrophotometry [13]. Plasma renin activity was measured by radio-immunoassay [14].

All data are expressed as the mean ± SE. Statistical analysis was performed by ANOVA using StatView 5 for Windows (SAS Institute Inc, NC). $P < 0.05$ was regarded as significant.

Results

All subjects completed the protocol without any complaints of taste disturbance. Mean blood pressure just before final dosing of the drug was not different between the three trials (110.5 ± 2.3, 108.1 ± 2.7 and 107.6 ± 2.5 mmHg, placebo, candesartan and valsartan, respectively). Figure 1 shows the recognition thresholds for sweetness using filter-paper disc at the end of the repeated treatment. It was significantly ($P < 0.05$) worsened after the repeated treatment of candesartan or valsartan, but not after placebo. The mean ± SE (and 95% CI) scores for the sweetness just before the 13th dosing

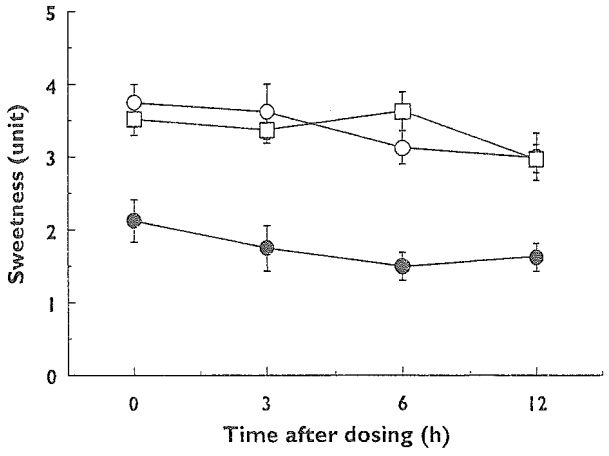

Figure 1
Detection thresholds for sweetness using filter-disc after the repeated dosing of candesartan, valsartan and placebo. Four basic tastes (sweet, salty, sour and bitter) were evaluated by using chemical solutions at the end of each treatment (day 14 + day 42 + day 70). A similar test was performed just before each protocol (day 1 + day 29 + day 57) and it was confirmed that the disturbances were completely improved after the washout period (data not shown). Mean ± SE, $n = 8$, Candesartan (○), Valsartan (□), Placebo (●)

Table 1
Difference of area under the time-score curve of tests, and time-concentration curve of zinc and plasma renin activity between drug and placebo

	Candesartan	Valsartan	95% CI
Sweet (U h^{-1})	15.75 ± 2.71	10.69 ± 2.43	(−6.15 to 16.27)
Salty (U h^{-1})	22.88 ± 5.16	19.75 ± 4.10	(−22.94 to 31.39)
Sour (U h^{-1})	11.06 ± 3.23	8.44 ± 2.69	(−11.74 to 16.99)
Bitter (U h^{-1})	12.94 ± 3.41	9.56 ± 2.39	(−12.43 to 19.68)
Electrogustometer (dB h^{-1})	42.98 ± 10.25	22.82 ± 11.41	(−10.67 to 50.93)
Salivary Zinc (mg dl^{-1} h^{-1})	−14.7 ± 10.8	−18.8 ± 14.5	(−10.2 to 8.9)
Serum Zinc (mg dl h^{-1})	−18.9 ± 20.2	−37.3 ± 33.5	(−24.2 to 15.5)
Plasma renin activity (ng ml^{-1})	182.1 ± 25.7	228.9 ± 34.2	(−18.5 to 50.7)

was 3.75 ± 0.25 (3.48–4.15), 3.53 ± 0.23 (3.19–3.94) and 2.13 ± 0.30 (1.75–2.55), for candesartan, valsartan and placebo, respectively. The detection thresholds of other three tastes were also significantly ($P < 0.05$) worsened after the repeated treatment of candesartan or valsartan, but not after placebo (data not shown). Difference of area under the time-score curve (determined by trapezoidal method) between a drug and placebo was shown in Table 1. The decrements of parameters were not different between candesartan and valsartan. The thresholds of the tastes just before each treatment were not different between the three groups (data not shown).

Detection thresholds at the end of each repeated treatment using an electrogustometer was also worsened by candesartan or valsartan to the same extent, but not by placebo (data not shown). Differences of area under the time-score curve (determined by trapezoidal method) between the drugs and placebo are shown in Table 1. The thresholds before each trial were not significantly different between the three groups (data not shown).

Salivary and serum zinc concentrations and plasma renin activity at the end of the repeated treatment were measured. Differences of area under the time–concentration curve (determined by trapezoidal method) between the drugs and placebo were shown in Table 1. Serum zinc concentration at 12 h after final dosing was significantly lower than other points in each trial. Plasma renin activity at the end of the repeated treatment was significantly higher in the trial with candesartan and valsartan than with placebo. However, no significant differences between the drug-treated groups were observed in these parameters.

Discussion

We measured plasma renin activity just before the taste test in this study because ARBs enhance plasma renin activity by the negative feedback after blocking angiotensin II receptor [15]. We found that both candesartan and valsartan at the doses used in this study (4 and 40 mg, respectively) increased this variable to a similar extent, which indicated that the treatment with candesartan and valsartan affected systemic renin-angiotensin-aldosterone axis to a similar degree. It is reported that 8 mg of candesartan and 80 mg of valsartan were equivalent to increment of plasma renin activity in healthy subjects [15], which is comparable to our study.

We compared two different ARBs on taste sensitivity in healthy subjects and found that the repeated oral dosing of candesartan and valsartan blunted taste sensitivity to a similar extent. To evaluate taste sensitivity, we used the same tests as our recent report [8] with a longer period of treatment from 7 to 13 days in this study. In addition, we found that the changes of the taste after the test were comparable for candesartan. Therefore, the alteration of taste reached a plateau in the earlier period of the treatment. In case reports of ARB-induced taste disturbance, patients noticed the problem from 1 week to 3 months after the initiation of the treatment with losartan [5, 6] and valsartan [7]. Based on our data and previous case reports, the taste disturbance might occur within a week, but patients needed several weeks to notice it.

We also measured serum zinc concentration because captopril disturbed taste sensitivity by chelating zinc in the body [3]. We found that both candesartan and valsartan did not change zinc concentration in serum and saliva, which is similar to our previous study using candesartan.

The mechanism of ARB-induced taste disturbance is not clear at the present time. Receptors for salt and sour in taste cell are elicited by ion channels [17] and may be affected by extra-cellular ion composition. Interest-

ingly, Lundy *et al.* proposed possible interaction of Na ion with the receptors [18]. Although we did not measure this parameter in serum and saliva, serum Na concentration is reduced by ARBs during the treatment in clinical situation [19]. It is uncertain that nerve conduction is disturbed. Further study is needed to solve this issue.

In summary, this study shows that the repeated dosing of candesartan and valsartan subclinically reduces the sensitivity of basic tastes in healthy subjects. The taste sensitivity was altered and plasma renin activity was elevated to the similar extent by both drugs. These results suggest that the taste disturbance-induced by candesartan is potentially similar to that of valsartan.

Competing interests: None declared.

References

1 Zegarelli D. Diseases of oral mucosa in Avery's drug treatment. (Ed. by Speight TN, Holford N). Auckland: Addis International, 1997 pp. 608–630.

2 Henkin RI. Drug-induced taste and smell disorders. Incidence, mechanisms and management related primarily to treatment of sensory receptor dysfunction. Drug Saf 1994; 11: 318–7.

3 Heyneman CA. Zinc deficiency and taste disorders. Ann Pharmacother 1996; 30: 186–7.

4 Tomita H, Yoshikawa T. Drug-related taste disturbances. Acta Otolaryngol Suppl 2002; 546: 116–2.

5 Schlienger RG, Saxer M, Haefeli WE. Reversible ageusia associated with losartan. Lancet 1996; 347: 471–2.

6 Heeringa M, van Puijenbroek EP. Reversible dysgeusia attributed to losartan. Ann Intern Med 1998; 129: 72.

7 Stroeder R, Zeissig L, RH. Angiotensin II-antagonist cGP48933 (valsartan), Ergebnisse einer doppelblinden, plazebo-Kontrolierten Multicenter-Studie. Nieren Hochdruckkrankheiten (in German) 1994; 23: 217–20.

8 Tsuruoka S, Wakaumi M, Nishiki K, Araki H, Harada K, Sugimoto K. Subclinical alteration of taste sensitivity induced by candesartan in healthy subjects. Br J Clin Pharmacol 2004; 57: 807–12.

9 Kuga M, Ikeda M. Evaluation of gustatory threshold changes in healthy subjects. Nippon Jibiinkoka Gakkai Kaiho 1996; 99: 411–6.

10 Tomita H, Ikeda M, Okuda Y. Basis and practice of clinical taste examinations. Auris Nasus Larynx 1986; 13(Suppl 1): S1–15.

11 Sato K, Endo S, Tomita H. Sensitivity of three loci on the tongue and soft palate to four basic tastes in smokers and non-smokers. Acta Otolaryngol Suppl 2002; 546: 74–82.

12 Tomita H, Ikeda M. Clinical use of electrogustometry: strengths and limitations. Acta Otolaryngol Suppl 2002; 546: 27–38.

13 Meret S, Henkin R. Simultaneous direct estimation by atomic absorption spectrophotometry of copper and zinc in serum, urine, and cerebrospinal fluid. Clin Chem 1971; 17: 369–73.

14 Heise CM. Letter: Measurement of plasma renin activity. Clin Chem 1975; 21: 447–9.

15 Maillard MP, Wurzner G, Nussberger J, Coteno C, Burniar M, Brunner HR. Comparative angiotensin II receptor blockade in healthy volunteers: the importance of dosing. Clin Pharmacol Ther 2002; 71: 68–76.

16 Favier A, Ruffieux D. Physiological variations of serum levels of copper, zinc, iron and manganese. Biomed Pharmacother 1983; 37: 462–6.

17 Lindemann B. Receptors and transduction in taste. Nature (Lond) 2001; 413: 219–25.

18 Lundy RF Jr. Potential mechanisms for functional changes in taste receptor cells following sodium deficiency in mammals. Neurosci Biobehav Rev 1998; 23: 103–9.

19 Higashiura K, Ura N, Miyazaki Y, Shimamoto K. Effect of an angiotensin II receptor antagonist, candesartan, on insulin resistance and pressor mechanisms in essential hypertension. J Hum Hypertens 1999; 13(Suppl 1): S71–4.

Artificial Organs
29(8):681–684, Blackwell Publishing, Inc.

Thoughts and Progress

The Bioreactor With CYP3A4- and Glutamine Synthetase-Introduced HepG2 Cells: Treatment of Hepatic Failure Dog With Diazepam Overdosage

*†‡Ning Wang, *Shuichi Tsuruoka, *Hisashi Yamamoto, §Shin Enosawa, ¶Takeshi Omasa, †Naohiro Sata, **Toshiharu Matsumura, †Hideo Nagai, and *Akio Fujimura

*Departments of *Clinical Pharmacology and †General Surgery, Jichi Medical School, Tochigi, Japan, ‡General Surgery Department II, China Medical University No. 1 Affiliated Hospital, Shenyang, China, §Department of Innovative Surgery, National Research Institute for Child Health and Development, Tokyo, ¶Department of Biotechnology, Graduate School of Engineering, Osaka University, Osaka, and **Cell Technology Center, Roman Industries Co. Ltd., Kanagawa, Japan*

Abstract: A novel recombinant human hepatic cell line, CYP3A4- and glutamine synthetase (GS, an enzyme which converts ammonium ion and glutamate to glutamine)-introduced HepG2 (HepG2-GS-CYP3A4), was established. Its usefulness in a large-scale culture with a circulatory bioreactor in vitro and in dog models of ischemic hepatic failure with acute diazepam (DZP, a substrate of CYP3A4) overdosage was further examined. HepG2-GS-CYP3A4 expressed about 9 times larger amounts of CYP3A4 protein than a control. After incubation with HepG2-GS-3A4 cells in a circulatory bioreactor for 24 h, ammonia and DZP concentrations in the culture medium significantly decreased by about 40%. Furthermore, this system improved the survival time and decreased serum concentrations of DZP, ammonia, and transaminase in dogs with ischemic hepatic failure plus acute DZP overdosage. The mean survival time with bioreactor with HepG2-GS-3A4 was 42.7 ± 3.6 h, which was significantly longer than that without reactor, with reactor (no cells), and with HepG2-GS (23.4 ± 2.8, 22.1 ± 2.4, and 31 ± 3.7 h, respectively). Therefore, it is concluded that this bioartificial liver could be a good tool for the treatment of dogs with hepatic failure and that it could potentially be a bridging procedure to liver transplantation. **Key Words:** Bioartificial liver—Diazepam intoxication—Hepatic failure—CYP3A4—HepG2—Dog.

Received November 2004; revised February 2005.

Address correspondence and reprint requests to Dr. Shuichi Tsuruoka, Department of Clinical Pharmacology, Jichi Medical School, 3311 Yakushiji Minamikawachi, Kawachi, Tochigi 329-0498, Japan. E-mail: tsuru@jichi.ac.jp

Hepatic failure leads to the accumulation of multiple water-insoluble toxins, such as unconjugated bilirubin and endogenous benzodiazepines (1). Especially, endogenous diazepam (DZP) and nordiazepam (NDZP) are considered to have a pivotal role in the pathogenesis of hepatic encephalopathy (2,3). Elimination half-life of DZP is five times longer in patients with liver cirrhosis than control subjects because the activity of cytochrome P450 3A4, a major metabolizing enzyme for this compound, is impaired. Therefore, providing metabolizing ability for DZP and other hepatic toxins is important for the treatment of hepatic failure.

A bioartficial liver (BAL) support system is expected to be a new tool for terminal-stage liver failure and for bridge-to-transplantation use (4). Enosawa et al. developed recombinant HepG2 cells with the introduction of glutamine synthetase (GS), an enzyme which converts ammonium ion and glutamate to glutamine, and applied them to a novel type of circulatory cell culture system (5,6). They reported significant removal of ammonia by this system in a hepatic failure model, but they could not achieve improvement in survival time in this model. These results indicate that some toxins other than ammonia are involved in hepatic failure, and intrinsic benzodiazepine might be a candidate.

The objectives of this study were: (i) to establish HepG2-GS-3A4 cells with the introduction of both GS and CYP3A4 genes; (ii) to assess the usefulness of HepG2-GS-3A4 cells in a BAL device in vitro; and (iii) to evaluate the system as a treatment modality for a canine model of acute hepatic failure combined with a DZP overdose.

METHODS

Cells and Western blot analysis for human cytochrome P450 3A4

HepG2 cells were obtained from the RIKEN cell bank (Tsukuba, Japan). HepG2-GS-3A4, a cell transfected with both the hamster GS gene and the human cytochrome p450 3A4 gene was established by lipofection of pBudCE4 (Invitrogen, Carlsbad, CA, U.S.A.) after ligation of both genes. A positive clone was selected by an index of resistant against zeocin. HepG2-GS-3A4 cells were cultured in DMEM/F-12: RPMI (1 : 1), with 10% FCS + zeocin. Twenty micro-

grams of protein was resolved by 7% SDS-PAGE electrophoresis, and immunoblotted with human CYP3A4 antibody (WB human CYP3A4 kit, BDGenetest, MA, U.S.A.).

Long-term culture in circulatory flow bioreactor for bioartficial liver (BAL) and treatment of acute hepatic failure with DZP overdosage

The circulatory flow bioreactor originally developed for culturing adhesive cells (US Patent no. 5270207) (5), was used as a bioartficial liver (6). During the culture, fresh culture medium, air, and CO_2 were continuously supplied to the vessel and the temperature was maintained at 37°C. Evaluation of the metabolizing capacity was performed at 20 days after inoculation of 1×10^8 cells. To evaluate metabolizing activity of DZP and ammonia, these compounds (2.5 mm and 30 μg/mL, respectively) were added to the fresh medium and the old medium flowing out from the reactor was sampled.

Beagle dogs (10–20 kg, $n = 23$) were anesthetized with pentobarbital (1 mg/kg, i.v.). The procedure of Abouna (7) was partly modified to establish an ischemic hepatic failure model with an end-to-side portal–vena cava shunt and ligation of hepatic arteries. One and half hours after operation, DZP was intravenously infused to each dog at a dose of 3 mg/kg. Blood samples were taken at scheduled times to check the level of ammonia, DZP, its metabolites, and aminotransferases. Dopamine (30 mg/kg/h at maximum dose) was infused to maintain arterial blood pressure. Termination of heartbeat was regarded as the end of survival.

Treatment with the bioartificial liver was performed just after the infusion of DZP. During the operation, culture medium was completely replaced with artificial solution for hemoperfusion and thereafter changed to 550 mL of dog plasma (6). A catheter was introduced into the femoral artery for drawing blood at 30–50 mL/min. The blood flowed into a plasma separator column (OP-02 W, Asahi Medical, Tokyo, Japan) and the separated plasma flowed into the BAL at a rate of 150–250 mL/h.

The concentrations of ammonia and transaminase were measured by modified Berthelot reaction and Reitman and Frankel's method (8) with autoanalyzer, respectively. Concentrations of DZP were measured by high-performance liquid chromatography (9). Values were expressed as the mean ± S.E. ANOVA and *t*-test were used as appropriate for statistical comparison. Survival rate for each treatment was compared by logrank analysis. $P < 0.05$ was regarded as significant.

RESULTS

Confirmation of human cytochrome P450 3A4 in HepG2-GS-3A4 cells and metabolism of ammonia and DZP in BAL system

The HepG2-GS-3A4 cells had about nine times higher amounts of CYP3A4 protein than HepG2 in Western blot analysis. Densitometric values were 0.18 ± 0.02 and 0.02 ± 0.01 units for HepG2-GS-3A4 and HepG2, respectively.

Concentrations of ammonia and DZP after incubation with HepG2-GS-3A4 cells in the bioreactor for 24 h are shown in Table 1. Ammonia and DZP concentrations significantly decreased with HepG2-GS-3A4 cells. HepG2-GS showed almost the same ammonia metabolism capacity as HepG2-GS-3A4 and caused nearly no DZP reduction. The initial removal rate of ammonia by the reactor with HepG2-GS-3A4 cells was about 0.4 nmol/min/10^6 cells. The amount of DZP metabolized by HepG2-GS-3A4 in the reactor, which was calculated from differences of the area under concentration-time curves between inlet and outlet of the medium and subtraction of the value obtained from the experiments, was significantly higher in HepG2-GS-3A4 (Table 1).

Treatment of acute hepatic failure with DZP loading by HepG2-GS-3A4 in the bioreactor

Treatment using the bioreactor with HepG2-GS-3A4 significantly prolonged survival time to 42.7 ± 3.6 h (Fig. 1). Treatment with HepG2-GS also prolonged mean survival time to 31 ± 3.7 h, but it did not reach statistical significance ($P = 0.08$). The time course of GPT, ammonia, and DZP are shown in Fig. 2. GPT and ammonia concentrations increased

TABLE 1. *Metabolism of ammonia and DZP by HepG2-GS-3A4 in the bioreactor in vitro*

	Concentration 24 h after incubation		Metabolized diazepam amount for 24 h (μg/hL)
	Ammonia (mM)	Diazepam (μg/mL)	
HepG2-GS-3A4 ($n = 4$)	1.5 ± 0.2**	19 ± 1*,**	74 ± 9*
HepG2-GS ($n = 3$)	2.0 ± 0.2**	23 ± 1	20 ± 10
Without cells ($n = 3$)	2.4 ± 0.2	24 ± 2	—

*$P < 0.05$ vs. HepG2-GS, **$P < 0.05$ vs. without cell.

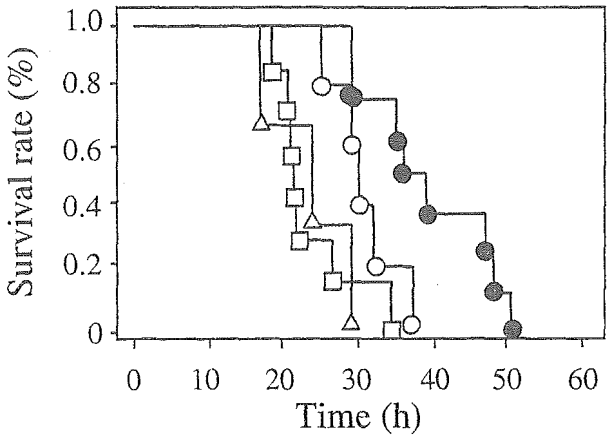

FIG. 1. Cumulative survival period for hepatic failure with DZP loading treated by a bioreactor with HepG2-GS-3A4. ● HepG2-GS-3A4 ($n = 8$); ○ HepG2-GS ($n = 5$); □ without cells ($n = 7$); △ without bioreactor (hepatic failure alone, $n = 3$).

with time in all groups, however, the increase at 24 h was less in the HepG2-GS-3A4 group for GPT and in both HepG2-GS-3A4 and HepG2-GS groups for ammonia. The reduction of DZP concentration was significantly more rapid in HepG2-GS-3A4 than other groups.

DISCUSSION

In this study, we clearly demonstrated the ability of HepG2-GS-3A4 cells in the bioreactor to metabolize DZP and ammonia. Thus, this is the first effective system that removes both DZP and ammonia, which accumulate in hepatic failure. In addition, this is the first report that shows the effectiveness of a system for removal of these molecules from circulating blood in an animal model. Although the clearance of ammonia and DZP was significant in our report, it still remains lower than normal hepatocytes. However, porcine hepatocytes have many disadvantages in a BAL system, such as xenoantigenicity, xenozoonosis, laborious handling, and difficulties in storage, although they have high capacity and multiple functions (6). As the HepG2-GS-3A4 cell line does not have any of these disadvantages, it is still a good candidate for the treatment of human hepatic failure.

When the acute hepatic failure dogs with DZP overdosage were treated using the bioreactor with HepG2-GS-3A4, DZP and ammonia concentrations were significantly reduced, and subsequently the survival period was significantly increased. This is the most important observation in this study. Similarly to the results of Enosawa, the reactor with HepG2-GS could decrease the plasma concentration of ammonia, but the survival period did not increase significantly (6). Although GPT was obviously lower during the treatment using the reactor with HepG2-GS-3A4, ammonia concentration with HepG2-GS-CYP3A4 did not differ from that of HepG2-GS. This observation suggests that toxins other than ammonia, which are metabolized by CYP3A4 such as endogenous benzodiazepins, are important for the mortality rate in hepatic failure. Although we did not measure intracranial pressure, the removal of intrinsic/extrinsic benzodiazepeins might reduce the pressure and prolong the survival. Alternatively, this BAL might not only help the dysfunctional liver to detoxify

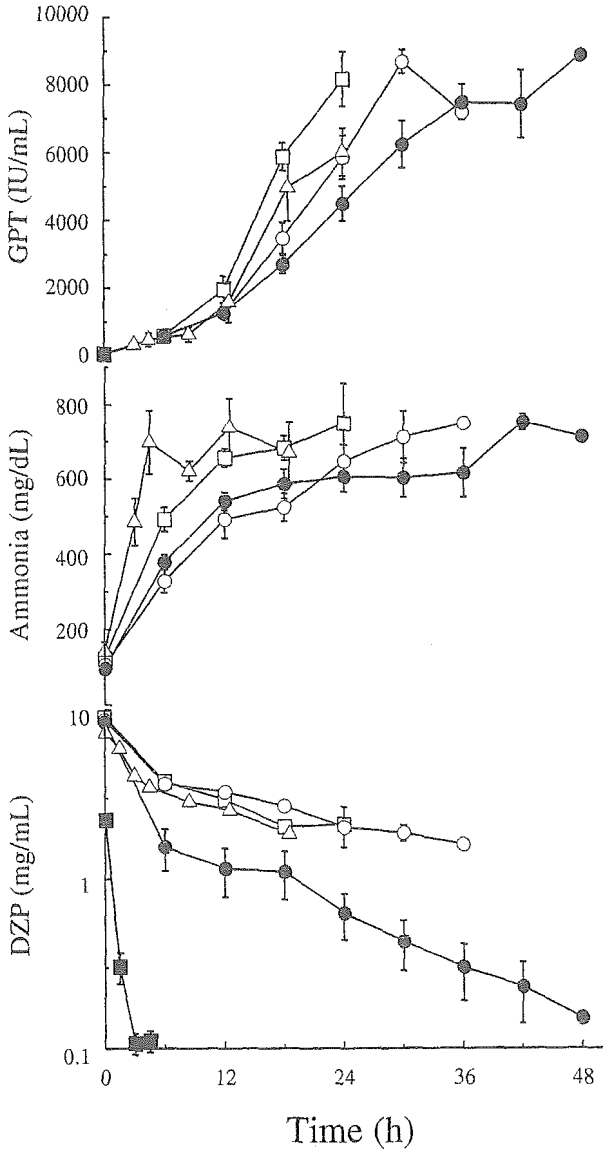

FIG. 2. Time course of GPT (upper panel), ammonia (middle panel), and DZP (lower panel) during treatment. ● HepG2-GS-3A4 ($n = 8$); ○ HepG2-GS ($n = 5$); □ without cells ($n = 7$); △ without bioreactor (hepatic failure alone, $n = 3$); ■ healthy dog ($n = 3$).

toxins, but it might also guard against destruction of hepatocytes.

In conclusion, the present study suggests that this system with HepG2-GS-3A4 can be potent for the treatment of dogs with hepatic failure when ammonia and endogenous benzodiazipines are high. This system might be useful as a bridge to liver transplantation, although more modification is needed to use it in clinical practice.

Acknowledgments: We thank Mr. S. Sato for his technical assistant. Part of this study was supported by Research on Advanced Medical Technology, Health and Labor Sciences Research Grants, and the Grant Program for Promoting Advancement of Academic Research at Private Universities, Ministry of Education, Culture, Science and Technology of Japan.

REFERENCES

1. Awad SS, Hemmila MR, Soldes OS, et al. A novel stable reproducible model of hepatic failure in canines. *J Surg Res* 2000;94:167–71.
2. Itzhak Y, Roig-Cantisano A, Dombro RS, et al. Acute liver failure and hyperammonemia increase peripheral-type benzodiazepine receptor binding and pregnenolone synthesis in mouse brain. *Brain Res* 1985;705:345–8.
3. Basile AS, Hughes RD, Harrison PM, et al. Elevated brain concentrations of 1,4-benzodiazepines in fulminant hepatic failure. *N Engl J Med* 1991;325:473–8.
4. Demetriou AA, Brown RS Jr, Busuttil RW, et al. Prospective, randomized, multicenter, controlled trial of a bioartificial liver in treating acute liver failure. *Ann Surg* 2004;239:660–70.
5. Matsumura T. United States Patent No. 5270207 1993.
6. Enosawa S, Miyashita T, Suzuki S, et al. Long-term culture of glutamine synthetase-transfected HepG2 cells in circulatory flow bioreactor for development of a bioartificial liver. *Cell Transplant* 2000;9:711–5.
7. Abouna GM, Ganguly PK, Hamdy HM, et al. Extracorporeal liver perfusion system for successful hepatic support pending liver regeneration or liver transplantation: a pre-clinical controlled trial. *Transplantation* 1999;67:1576–83.
8. Reitman S, Frankel S. A colorimetric method for the determination of serum glutamic oxalacetic and glutamic pyruvic transaminases. *Am J Clin Pathol* 1957;28:56–63.
9. Azzam RM, Notarianni LJ, Ali HM. Rapid and simple chromatographic method for the determination of diazepam and its major metabolites in human plasma and urine. *J Chromatogr B Biomed Sci Appl* 1998;708:304–9.

0013-7227/05/$15.00/0
Printed in U.S.A.

Endocrinology 146(12):5631–5636

doi: 10.1210/en.2005-0771

Rhythmic Messenger Ribonucleic Acid Expression of Clock Genes and Adipocytokines in Mouse Visceral Adipose Tissue

Hitoshi Ando, Hayato Yanagihara, Yohei Hayashi, Yuri Obi, Shuichi Tsuruoka, Toshinari Takamura, Shuichi Kaneko, and Akio Fujimura

Division of Clinical Pharmacology (H.A., H.Y., Y.H., Y.O., S.T., A.F.), Department of Pharmacology, Jichi Medical School, Tochigi 329-0498, Japan; and Department of Diabetes and Digestive Disease (T.T., S.K.), Kanazawa University Graduate School of Medical Science, Kanazawa, Ishikawa 920-8641, Japan

Various peripheral tissues show circadian rhythmicity, which is generated at the cellular level by their own core oscillators that are composed of transcriptional/translational feedback loops involving a set of clock genes. Although the circulating levels of some adipocytokines, *i.e.* bioactive substances secreted by adipocytes, are on a 24-h rhythmic cycle, it remains to be elucidated whether the clock gene system works in adipose tissue. To address this issue, we investigated the daily mRNA expression profiles of the clock genes and adipocytokines in mouse perigonadal adipose tissues. In C57BL/6J mice, all transcript levels of the clock genes (Bmal1, Per1, Per2, Cry1, Cry2, and Dbp) and adipocytokines (adiponectin, resistin, and visfatin) clearly showed 24-h rhythms. On the other hand, the rhythmic expression of these genes was mildly attenuated in obese KK mice and greatly attenuated in more obese, diabetic KK-A^y mice. Obese diabetes also diminished the rhythmic expression of the clock genes in the liver. Interestingly, a 2-wk treatment of KK and KK-A^y mice with pioglitazone impaired the 24-h rhythmicity of the mRNA expression of the clock genes and adipocytokines despite the antidiabetic effect of the drug. In contrast, pioglitazone improved the attenuated rhythmicity in the liver. These findings suggest that the intracellular clock gene system acts in visceral adipose tissues as well as liver and is influenced by the conditions of obesity/type 2 diabetes and pioglitazone treatment. (*Endocrinology* 146: 5631–5636, 2005)

VARIOUS PHYSIOLOGICAL and behavioral processes exhibit circadian rhythmicity. Recent studies have revealed that these endogenous rhythms are generated at the cellular level by circadian core oscillators, which are composed of transcriptional/translational feedback loops involving a set of clock genes (1–3). In mammals, rhythmic transcriptional enhancement by two basic helix-loop-helix PER-ARNT-SIM domain-containing transcription factors, CLOCK and brain and muscle ARNT-like protein (BMAL)1, provides the basic drive to the system; the CLOCK-BMAL1 heterodimer directly or indirectly activates the transcription of various clock-controlled genes (1–5). For example, the albumin D-site binding protein (Dbp), which expression is directly regulated by the CLOCK-BMAL1, is involved in the circadian transcriptional regulation of several metabolic enzymes (1–3). In parallel, the heterodimer activates the transcription of several clock genes, including period (PER) and cryptochrome (CRY) (6–8). The resultant PER and CRY proteins translocate back into the nucleus and inhibit the activity of CLOCK-BMAL1, forming the negative feedback loop (1–3, 9). Thus, these clock genes control the circadian rhythm of physiological output by regulating the expression of multiple clock-controlled genes.

The intracellular circadian clock system resides in not only the hypothalamic suprachiasmatic nucleus, which is recognized as being the mammalian central clock, but also various peripheral tissues (10–12). The suprachiasmatic nucleus is not essential for driving peripheral oscillations but rather acts as a synchronizer of peripheral oscillators (12). Therefore, the physiological rhythmicity in peripheral tissues may be controlled directly by their own clock genes.

Recent advances in the understanding of adipocyte biology have indicated that adipose tissue not only serves as an energy-storing tissue but also performs a secretory function by producing a variety of bioactive substances, including adiponectin, resistin, and leptin, thus acting as endocrine tissue (13). Because some of these so-called adipocytokines greatly influence insulin sensitivity, glucose metabolism, and atherosclerosis, they may provide a molecular link between the increased adiposity and development of type 2 diabetes and/or metabolic syndrome (14). Among these adipocytokines, the circulating level of leptin exhibits a clear diurnal variation in animals (15–17) and humans (18–20). Moreover, plasma adiponectin concentrations in nonobese subjects show a 24-h rhythmic cycle, which is absent in obese subjects (19, 20). In addition, altered expression of the clock genes Per2 and Bmal1 has been reported in the livers of db/db mice, which serve as a model of severe, obese diabetes (21). Therefore, it is possible that clock genes in adipose tissue regulate the expression and/or secretion of adipocytokines and that obesity leading to insulin resistance and type 2

First Published Online September 15, 2005

Abbreviations: BMAL, Brain and muscle ARNT-like protein; CRY, cryptochrome; Dbp, albumin D-site binding protein; GAPDH, glyceraldehyde-3-phosphate dehydrogenase; PER, period; PLSD, protected least significant differences; PPAR, peroxisome proliferators-activated receptor; ZT, zeitgeber time.

Endocrinology is published monthly by The Endocrine Society (http://www.endo-society.org), the foremost professional society serving the endocrine community.